



CHORUS

This is the accepted manuscript made available via CHORUS. The article has been published as:

Observation of Defect States in PT-Symmetric Optical Lattices

Alois Regensburger, Mohammad-Ali Miri, Christoph Bersch, Jakob Näger, Georgy Onishchukov, Demetrios N. Christodoulides, and Ulf Peschel

Phys. Rev. Lett. **110**, 223902 — Published 29 May 2013

DOI: [10.1103/PhysRevLett.110.223902](https://doi.org/10.1103/PhysRevLett.110.223902)

Observation of Defect States in \mathcal{PT} -Symmetric Optical Lattices

Alois Regensburger^{†,1}, Mohammad-Ali Miri^{†,2}, Christoph Bersch,¹ Jakob Näger,¹
Georgy Onishchukov,³ Demetrios N. Christodoulides,² and Ulf Peschel^{1,*}

¹*Institute of Optics, Information and Photonics, SAOT,
University of Erlangen-Nuernberg, 91058 Erlangen, Germany*

²*CREOL/College of Optics, University of Central Florida, Orlando, Florida 32816, USA*

³*Max Planck Institute for the Science of Light, 91058 Erlangen, Germany*

We provide the first experimental demonstration of defect states in parity-time (\mathcal{PT}) symmetric mesh-periodic potentials. Our results indicate that these localized modes can undergo an abrupt phase transition in spite of the fact that they remain localized in a \mathcal{PT} -symmetric periodic environment. Even more intriguing is the possibility of observing a linearly growing radiation emission from such defects provided their eigenvalue is associated with an exceptional point that resides within the continuum part of the spectrum. Localized complex modes existing outside the band-gap regions are also reported along with their evolution dynamics.

PACS numbers: 42.81.Qb, 42.25.Bs 11.30.Er

Defects play a crucial role in determining the physical and chemical properties of solids [1]. In semiconductor crystals, the presence of defects leads to both bulk and surface electronic states that ultimately affect charge transport processes. When analyzed from the viewpoint of their corresponding band structure, such localized quantum eigenstates are known to reside within the forbidden energy gaps. In optics, similar effects are also possible in photonic crystal arrangements which have been so far exploited to realize high quality dielectric waveguides and cavity resonators [2–4]. In most cases, such defect modes have been investigated within the context of Hermitian systems. Yet, much less is known about the physics and properties of defects in non-Hermitian periodic configurations where the vector space is no longer orthogonal but is instead skewed. In the optical domain, non-hermiticity can be readily introduced through either amplification or loss. Such arrangements include for example defect mode lasers in photonic band-gap crystals [5], photonic crystal fiber amplifiers [6] and semiconductor distributed-feedback lasers [7]. The spectrum of these latter systems is in general complex, allowing only some of the modes to enjoy amplification.

Lately, the notion of parity-time (\mathcal{PT}) symmetry has been introduced in optics as a new paradigm to mold the flow of light [8, 9]. This idea, which originated within the context of quantum field theories [10, 11], has led to new strategies in achieving a harmonic interplay between optical gain and loss. In general, a necessary (but not sufficient) condition for an optical structure to be \mathcal{PT} -symmetric is that its complex refractive index distribution satisfies the condition $n(x) = n^*(-x)$, in which case the real part of the index profile is expected to be symmetric in space while the imaginary component (gain-loss) is antisymmetric. Optical systems endowed with this symmetry are known to exhibit altogether real spectra. \mathcal{PT} symmetry can lead to unusual and previously unattainable light propagation features [9, 12–

24]. These include double refraction and band merging [8, 12], abrupt phase transitions and power oscillations [16, 17], unidirectional invisibility [23] and non-reciprocal propagation [19], as well as coexistence of coherent lasing-absorbing modes and mode selection in \mathcal{PT} -symmetric lasers [9, 20, 21]. Quite recently, light transport in large-scale temporal \mathcal{PT} -symmetric mesh lattices has been reported [12, 13]. Given that the band structure of a \mathcal{PT} -symmetric lattice can be entirely real, one could ask in what fundamental ways the properties of a defect state will be altered in such a pseudo-Hermitian environment.

In this Letter, we report the first experimental observation of defect states in \mathcal{PT} -symmetric lattices [Fig. 1(a)]. We demonstrate the transition from stable to exponentially growing bound modes while their localization properties remain preserved. Furthermore, we show that for a defect state in its broken symmetry regime, the corresponding eigenvalue does not necessarily have to reside within the band gap region—as in conventional Hermitian periodic structures. Finally, at \mathcal{PT} threshold, we observe a stable parity-time symmetric defect mode that constantly emits coherent radiation to the surrounding lattice at a linear growth rate.

The experimental setup in Fig. 1(b) [12, 25, 26] consists of two loops of optical fiber which are connected by a 50:50 coupler. A length difference of ΔL between the loops enables a temporal advancement or delay of the light pulses in every round trip [26, 27]. The required refractive index distribution in this arrangement is realized using a phase modulator in one of the loops. Additionally, the antisymmetric imaginary part of the photonic potential is implemented by temporally switching gain and loss between the two loops. A comprehensive technical documentation is provided in the Supplemental Material [25]. One can show that the resulting pulse dynamics in this system is governed by the following dif-

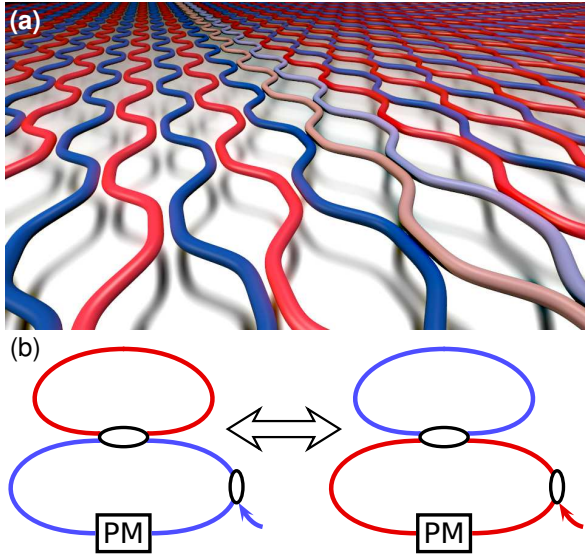


FIG. 1. (Color online). (a) Equivalent spatial waveguide mesh lattice corresponding to the temporal fiber loop scheme used in the experiments shown in (b). Red and blue waveguides indicate balanced regions of gain and loss while transverse 50% coupling takes place where waveguides come close. A pair of waveguides with a different gain-loss contrast and/or phase shift acts as a defect. (b) Coupled fiber loops used in the experiment. PM: phase modulator.

ference equations [12, 26]:

$$\begin{aligned} u_n^{m+1} &= \frac{1}{\sqrt{2}} \tilde{G}(n+1)^{\frac{1}{2}(-1)^m} (u_{n+1}^m + i v_{n+1}^m) \\ v_n^{m+1} &= \frac{1}{\sqrt{2}} \tilde{G}(n)^{-\frac{1}{2}(-1)^m} (i u_{n-1}^m + v_{n-1}^m) e^{i\tilde{\varphi}(n)}. \end{aligned} \quad (1)$$

Here, u_n^m and v_n^m are the amplitudes of light pulses circulating in the short and long loop, respectively. m corresponds to the number of round trips and n accounts for the transverse temporal position of a pulse. As indicated in Ref. [25], Eqs. (1) can be transformed into standard form associated with mesh lattices [13].

The phase potential $\tilde{\varphi}(n) = \tilde{\varphi}_p(n) + \tilde{\varphi}_d(n)$ consists of a periodic part $\tilde{\varphi}_p = \begin{cases} +\varphi_p & \text{for } \text{mod}(n, 4) = 0, 1 \\ -\varphi_p & \text{for } \text{mod}(n, 4) = 2, 3 \end{cases}$, and the phase defect $\tilde{\varphi}_d(n)$ which takes the value φ_d for n within the defect and is 0 elsewhere.

In our setup, from one round trip to another, gain and loss alternate between the loops. In general, the gain factor $\tilde{G}(n) = G_p + \tilde{G}_d(n)$ itself can depend on n : $\tilde{G}_d(n)$ takes the value G_d for n inside the defect and is 0 everywhere else, thus creating a defect in the imaginary part of the effective potential. In the experiment, the same transverse profiles for the gain and phase potential are used for every loop round trip m .

Before introducing defects in a \mathcal{PT} -symmetric optical mesh lattice, we first investigate the corresponding passive Hermitian system [28]. Consider an elemental phase

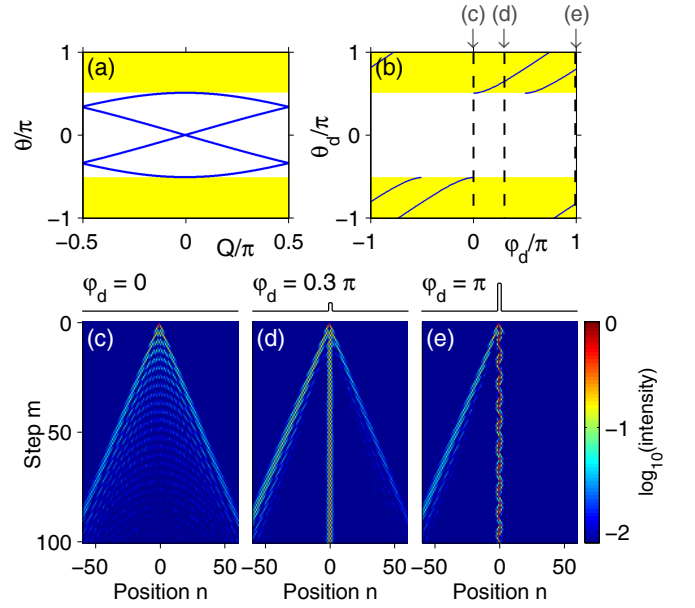


FIG. 2. (Color online). Phase defect in a passive mesh lattice. (a) The band structure of the empty lattice ($G_p = 1$, $\varphi_p = 0$) relates the transverse wave number Q and the propagation constant θ . The yellow regions denote band gaps [13]. (b) Dispersion curves of the defect modes as a function of the defect phase φ_d . Experimental results for the evolution of a single pulse in this lattice with a phase defect of strength φ_d where (c) $\varphi_d = 0$ (no defect), (d) $\varphi_d = 0.3\pi$, (e) $\varphi_d = \pi$. The total phase potential $\tilde{\varphi}(n)$ is also indicated for each case. In all cases only data from the short loop (u_n^m) is displayed [25].

defect φ_d at positions $n = \{0, 1\}$ in a passive environment ($G_p = 1$) where no background potential is present ($\varphi_p = 0$). In the absence of a defect, the band structure [13] has two connected bands, with the photonic band gaps positioned above and below [Fig. 2(a)] in its reduced Brillouin zone. This can be obtained via a plane wave ansatz of the form $e^{iQn/4} e^{i\theta m/2}$, where Q and θ represent the transverse Bloch momentum and propagation constants respectively. Such calculations are explained in detail in Refs. [13, 25]. The propagation of light pulses in this configuration is classically analogous [26] to a quantum walk [27–30], as can be seen in Fig. 2(c). Depending on the defect phase φ_d , either one or two localized modes can exist inside the band gap [Fig. 2(b)]. In our experiment, we inject a single pulse into the long loop which is then monitored during propagation. A convolution of this delta-like impulse with the localized defect states as well as any continuum modes within the bands determines the weights of mode excitation. In the Hermitian system, the strength of each mode remains invariant during propagation. As defect modes are indeed excited, we observe a clear localization of light along the phase defect [Figs. 2(d,e)]. For $\varphi_d = \pi$, an oscillatory intensity pattern reveals the presence of two defect modes which continuously interfere with each other. The period of

this beating in Fig. 2(e) is close to 10 steps in m , which is compatible with the difference between the two associated propagation constants $\Delta\theta_d \approx 0.4\pi = \frac{2}{10}2\pi$.

A more complex behavior arises when the same defect is introduced into a \mathcal{PT} -symmetric mesh lattice having a balanced optical gain-loss profile ($G_p = 1.3$) and a periodic phase (refractive index) potential ($\varphi_p = 0.2\pi$). Given that the periodic lattice parameters G_p and φ_p were chosen to be below the \mathcal{PT} threshold of this lattice ($\ln(G_p) < \cosh^{-1} [2 \cos(\varphi_p) - \sqrt{\cos(2\varphi_p)}]$) [12, 13], in the absence of a defect, the band structure of this non-Hermitian system is entirely real [Fig. 3(a,c)]. In this manner none of the Floquet-Bloch modes can grow exponentially. In what follows, we will only consider defects that satisfy the \mathcal{PT} condition of $n(x) = n^*(-x)$ in the entire system (lattice plus defect).

We now introduce a similar phase defect into a \mathcal{PT} lattice while the imaginary part of the combined \mathcal{PT} potential remains completely periodic. As predicted by our theoretical results, [Fig. 3(b)], a transition between almost stable localized modes with real propagation constants and exponentially growing bound states with complex eigenvalues is possible, which is in fact observed [Fig. 3(d,e)] in our experiments. Indeed, in the latter case, a pair of defect modes with broken \mathcal{PT} symmetry (complex eigenvalues) emerges. Remarkably, this transition happens when increasing the defect potential φ_d while the gain-loss G_p and background potential φ_p are kept constant, see Fig. 3(a). This is counterintuitive given that for a homogeneous lattice, such an increase in the optical potential's real part typically leads to stabilization [12].

Thus far, the propagation constants θ_d of the bound defect modes were all found to lie within the band gap of the periodic structure, thus prohibiting any coupling to phase-matched free propagating radiation modes. Note that the only way bound states can exist inside the continuum of bands (in Hermitian systems) is when they are totally decoupled from their surroundings by virtue of some special symmetry [32, 33].

As we will see, in stark contrast to Hermitian systems, in the case of \mathcal{PT} lattices defect states with complex eigenvalues can also appear within the band continuum. If a defect possesses an imaginary G_d component (in addition to the real part φ_d) which differs from the periodic gain-loss G_p profile, then it is possible to establish localized modes having propagation constants whose real parts $\text{Re}(\theta_d)$ are located inside the bands. In this regime, the inherent gain of the system compensates for light leaking away (because of phase-matching) into lattice radiation modes. These defect modes have a non-zero imaginary part $\text{Im}(\theta_d)$ that reveals itself through exponential growth or decay. Despite the fact that their coupling to the continuum is not inhibited, these \mathcal{PT} localized states still decay exponentially on both sides. Essentially, this

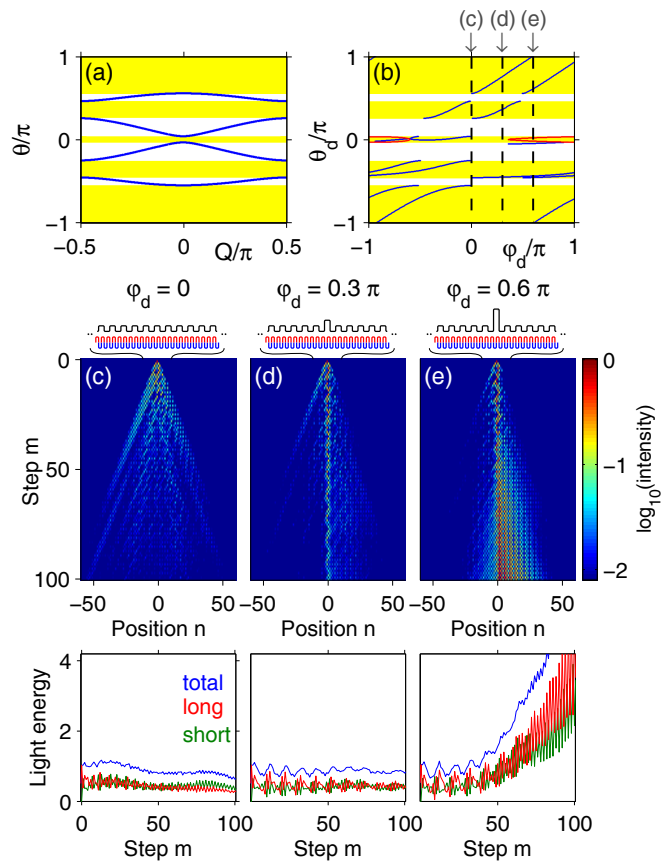


FIG. 3. (Color online). Phase defect in a \mathcal{PT} -synthetic lattice. (a) Real band structure of the background \mathcal{PT} lattice (below threshold) with a gain-loss $G_p = 1.3$ and a phase potential $\varphi_p = 0.2\pi$. (b) Dispersion diagram of defect states as a function of defect phase φ_d . Here, real and imaginary parts are shown in blue and red respectively. (c) Measurement of single pulse evolution when $\varphi_d = 0$ (no defect) and for (d) $\varphi_d = 0.3\pi$. In this last case, bound modes with real propagation constants θ_d are observed. (e) Increasing φ_d to 0.6π brings a pair of bound modes above the \mathcal{PT} threshold. The real ($\tilde{\varphi}(n)$) and imaginary ($\tilde{G}(n)$) parts of the \mathcal{PT} potentials as well as the evolution of the total power are indicated.

exponential localization is a direct outcome of the exponential increase a defect mode experiences in time.

In order to observe such defect states in optical mesh lattices, we introduce a broad \mathcal{PT} -symmetric defect in a background empty lattice ($G_p = 1$ and $\varphi_p = 0$). The defect region extends over 14 discrete positions n and possesses a gain-loss contrast of $G_d = 1.3$ and a defect phase of $\varphi_d = 0.2\pi$, see Ref. [25]. This extended defect allows one to observe these effects at experimentally attainable gain-loss values. According to the dispersion diagram of Fig. 4(a), this lattice can in general support several defect modes. In the range of $0 < |\varphi_d| < 0.5\pi$, a pair of defect states with complex conjugate eigenvalues (one growing while the other one decaying) is found to exist in spite of the fact that their corresponding real part

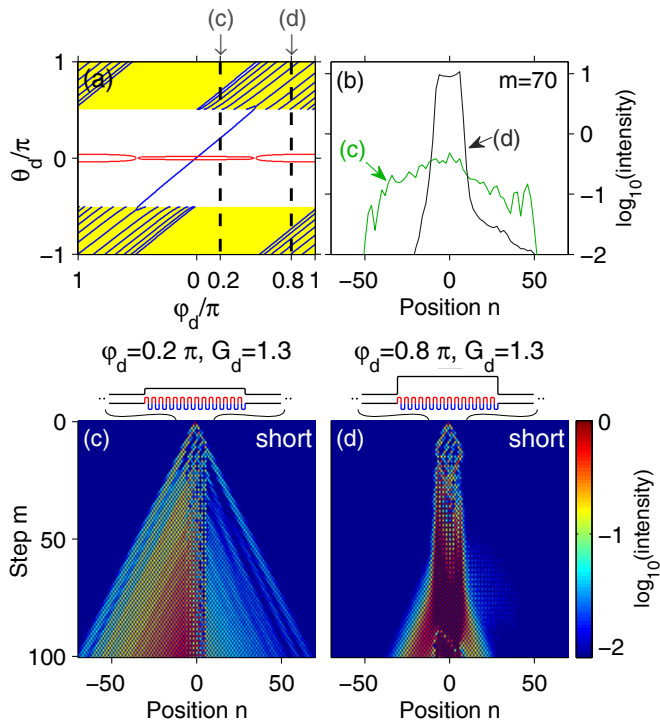


FIG. 4. (Color online). Defect modes residing in the continuum. (a) Dispersion diagram of a broad \mathcal{PT} -symmetric defect when embedded into an empty lattice. Apart from several other defect modes having real eigenvalues and located in the band gap (yellow region), for $\varphi_d < 0.5\pi$ this structure also supports a pair of localized modes with complex θ_d , that lie inside the continuum. (b) Pulse intensity profiles after $m = 70$ steps of propagation. (c) Observation of a growing weakly localized mode in the continuum for $\varphi_d = 0.2\pi$. (d) Increasing φ_d to 0.8π brings the mode into the band gap, leading to strong localization.

resides inside the band continuum. In our experiment, by choosing $\varphi_d = 0.2\pi$ we clearly observe this weakly localized exponentially growing defect state [Figs. 4(b,c)]. When increasing the defect's real potential φ_d to 0.8π , this pair of complex defect eigenmodes migrates into the band gap thus becoming tightly bound to the defect site [Fig. 4(d)] while it still grows/decays exponentially.

Even more surprising is how in this same structure, the gain-loss coefficient G_d ultimately affects the properties of these complex defect states. According to Fig. 5(a), when G_d decreases (for $\varphi_d = 0.2\pi$), the defect eigenvalue spectrum becomes again real and hence the total energy in the lattice remains bounded. However, right at the transition threshold which corresponds to $G_d = 1.25$, the mode is no longer exponentially localized and the total light power in the lattice now grows linearly while the rest of the defect eigenvalues are still real [Fig. 5(b)]. In this case, the pulse intensity within the active defect region oscillates around a stable mean value, while the structure constantly emits optical power toward both sides, see Figs. 5(c,d). This can be understood from Fig. 5(a)

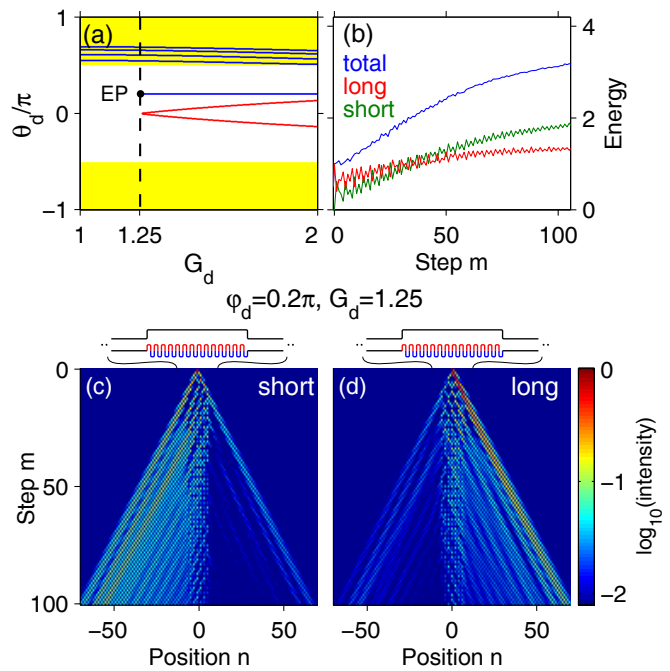


FIG. 5. (Color online). A defect mode at its exceptional point (EP). (a) Dispersion diagram of defect modes existing in the same structure as in Fig. 4 with $\varphi_d = 0.2\pi$ and as a function of G_d . According to this plot \mathcal{PT} threshold occurs at $G_d \approx 1.25$. (b) Measured light energy and (c,d) propagation in short and long loops at $G_d \approx 1.25$, confirming an almost linear growth in total energy and a continuous emission of power.

which clearly indicates the presence of an exceptional point within the band. Here a transition occurs between a pair of radiation modes (with real eigenvalues) and two localized complex modes endowed with a finite norm. Therefore, it is possible to create a continuously emitting coherent light source within a photonic lattice by embedding an appropriately designed gain-loss defect, as demonstrated in our experiment [Fig. 5(c)], which indeed confirms a linear growth of total light power [Fig. 5(b)]. Note that a similar behavior occurs in active Fabry-Perot cavities when operated at lasing threshold; in this regime, when gain is exactly equal to the total loss, power remains constant within the cavity while coherent laser light constantly flows toward the outside environment, with the total energy growing linearly [34].

In conclusion, we have investigated, both theoretically and experimentally, the properties of complex defects in \mathcal{PT} -symmetric optical lattices. We have shown that defect modes in such structures can exhibit extraordinary characteristics that are by no means attainable in standard Hermitian systems. Among them is the prospect of \mathcal{PT} -symmetry breaking instabilities and the possibility of establishing localized complex defect modes with spectra lying within the band continuum. In such \mathcal{PT} -symmetric environments, not only light beams can be trapped within a defect, but can also be controlled at

will through a defect parameter—thus altering the respective power emission characteristics to the surrounding regions. Our results may lead to new possibilities in judiciously structuring gain and loss in optical lattices that could in turn be potentially useful in lasing systems and other optical structures and devices.

We acknowledge financial support from DFG Forschergruppe 760, the Cluster of Excellence Engineering of Advanced Materials and the German-Israeli Foundation. This work was also supported by NSF grant ECCS-1128520 and by AFOSR grant FA95501210148. Moreover, we thank M. Wimmer for discussions.

* ulf.peschel@physik.uni-erlangen.de; †: Equal contribution.

- [1] N. W. Ashcroft and N. D. Mermin, *Solid State Physics*, edited by F. Seitz and D. Turnbull (Brooks Cole, 1976) Chap. 4.
- [2] A. Mekis, J. Chen, I. Kurland, S. Fan, P. Villeneuve, and J. Joannopoulos, *Phys. Rev. Lett.* **77**, 3787 (1996).
- [3] E. Yablonovitch, T. Gmitter, R. Meade, A. Rappe, K. Brommer, and J. Joannopoulos, *Phys. Rev. Lett.* **67**, 3380 (1991).
- [4] H. Trompeter, U. Peschel, T. Pertsch, F. Lederer, U. Streppel, D. Michaelis, and A. Bräuer, *Opt. Express* **11**, 3404 (2003).
- [5] O. Painter, R. K. Lee, A. Scherer, A. Yariv, J. L. O'Brien, P. Dapkus, and I. Kim, *Science* **284**, 1819 (1999).
- [6] J. C. Knight, J. Broeng, T. Birks, and P. S. J. Russell, *Science* **282**, 1476 (1998).
- [7] H. A. Haus, *Waves and fields in optoelectronics* (Prentice-Hall, 1984).
- [8] K. G. Makris, R. El-Ganainy, D. N. Christodoulides, and Z. H. Musslimani, *Phys. Rev. Lett.* **100**, 103904 (2008); Z. H. Musslimani, K. G. Makris, R. El-Ganainy, and D. N. Christodoulides, *ibid.* **100**, 030402 (2008).
- [9] R. El-Ganainy, K. G. Makris, D. N. Christodoulides, and Z. H. Musslimani, *Opt. Lett.* **32**, 2632 (2007); M.-A. Miri, P. LiKamWa, and D. N. Christodoulides, *ibid.* **37**, 764 (2012).
- [10] C. M. Bender and S. Boettcher, *Phys. Rev. Lett.* **80**, 5243 (1998); C. M. Bender, D. C. Brody, and H. F. Jones, *ibid.* **89**, 270401 (2002); C. M. Bender, *Rep. Prog. Phys.* **70**, 947 (2007).
- [11] A. Mostafazadeh, *J. Math. Phys.* **43**, 205 (2002); G. Lévai and M. Znojil, *J. Phys. A: Math. Gen.* **33**, 7165 (2000); Z. Ahmed, *Phys. Lett. A* **282**, 343 (2001).
- [12] A. Regensburger, C. Bersch, M.-A. Miri, G. Onishchukov, D. N. Christodoulides, and U. Peschel, *Nature (London)* **488**, 167 (2012).
- [13] M.-A. Miri, A. Regensburger, U. Peschel, and D. Christodoulides, *Phys. Rev. A* **86**, 023807 (2012).
- [14] Y. N. Joglekar, D. Scott, M. Babbey, and A. Saxena, *Phys. Rev. A* **82**, 030103 (2010).
- [15] E.-M. Graefe and H. Jones, *Phys. Rev. A* **84**, 013818 (2011).
- [16] C. E. Rüter, K. G. Makris, R. El-Ganainy, D. N. Christodoulides, M. Segev, and D. Kip, *Nat. Physics* **6**, 192 (2010); A. Guo, G. J. Salamo, M. Volatier-Ravat, V. Aimez, G. A. Siviloglou, and D. N. Christodoulides, *Phys. Rev. Lett.* **103**, 093902 (2009).
- [17] S. Klaiman, U. Günther, and N. Moiseyev, *Phys. Rev. Lett.* **101**, 080402 (2008).
- [18] B. Midya, B. Roy, and R. Roychoudhury, *Phys. Lett. A* **374**, 2605 (2010).
- [19] H. Ramezani, T. Kottos, R. El-Ganainy, and D. Christodoulides, *Phys. Rev. A* **82**, 043803 (2010); O. Bendix, R. Fleischmann, T. Kottos, and B. Shapiro, *Phys. Rev. Lett.* **103**, 030402 (2009).
- [20] Y. Chong, L. Ge, and A. Stone, *Phys. Rev. Lett.* **106**, 093902 (2011); M. Liertzer, L. Ge, A. Cerjan, A. Stone, H. Türeci, and S. Rotter, *ibid.* **108**, 173901 (2012).
- [21] H. Schomerus, *Phys. Rev. Lett.* **104**, 233601 (2010).
- [22] S. Longhi, *Phys. Rev. Lett.* **103**, 123601 (2009); *Phys. Rev. A* **82**, 031801 (2010).
- [23] Z. Lin, H. Ramezani, T. Eichelkraut, T. Kottos, H. Cao, and D. Christodoulides, *Phys. Rev. Lett.* **106**, 213901 (2011); M. Kulishov, J. M. Laniel, N. Bélanger, J. Azaña, and D. V. Plant, *Opt. Express* **13**, 3068 (2005); L. Feng, Y.-L. Xu, W. S. Fegadolli, M.-H. Lu, J. E. B. Oliveira, V. R. Almeida, Y.-F. Chen, and A. Scherer, *Nature Materials* **12**, 108 (2012).
- [24] A. Miroshnichenko, B. Malomed, and Y. Kivshar, *Phys. Rev. A* **84**, 012123 (2011); S. Suchkov, S. Dmitriev, B. Malomed, and Y. Kivshar, **85**, 033825 (2012).
- [25] Supplementary material [link to be inserted].
- [26] A. Regensburger, C. Bersch, B. Hinrichs, G. Onishchukov, A. Schreiber, C. Silberhorn, and U. Peschel, *Phys. Rev. Lett.* **107**, 233902 (2011).
- [27] A. Schreiber, K. N. Cassemiro, V. Potoček, A. Gábris, P. J. Mosley, E. Andersson, I. Jex, and C. Silberhorn, *Phys. Rev. Lett.* **104**, 050502 (2010); A. Schreiber, A. Gábris, P. P. Rohde, K. Laiho, M. Štefaňák, V. Potoček, C. Hamilton, I. Jex, and C. Silberhorn, *Science* **336**, 55 (2012).
- [28] A. Wojcik, T. Luczak, P. Kurzynski, A. Grudka, T. Gdala, and M. Bednarska-Bzdega, *Phys. Rev. A* **85**, 012329 (2012).
- [29] D. Bouwmeester, I. Marzoli, G. Karman, W. Schleich, and J. Woerdman, *Phys. Rev. A* **61**, 013410 (1999).
- [30] L. Sansoni, F. Sciarrino, G. Vallone, P. Mataloni, A. Crespi, R. Ramponi, and R. Osellame, *Phys. Rev. Lett.* **108**, 010502 (2012).
- [31] The Brillouin zone is defined over two steps m [13].
- [32] Y. Plotnik, O. Peleg, F. Dreisow, M. Heinrich, S. Nolte, A. Szameit, and M. Segev, *Phys. Rev. Lett.* **107**, 183901 (2011); M. Molina, A. Miroshnichenko, and Y. Kivshar, **108**, 070401 (2012).
- [33] H. Friedrich and D. Wintgen, *Phys. Rev. A* **32**, 3231 (1985).
- [34] A. Siegman, *Lasers* (University Science Books, 1986).